# THE PHYSICS AND EQUIVALENT CIRCUIT OF THE BASIC SAW RESONATOR*

R.C.M. Li, J.A. Alusow and R.C. Williamson
Lincoln Laboratory, Massachusetts Institute of Technology
Lexington, Massachusetts 02173

## Abstract

The physics of the basic surface-acoustic wave (SAW) resonator, together with factors which limit its achievable Q, are reviewed. Analogies to conventional microwave resonators are noted, and microwave-network techniques employed in their analysis and design are discussed.

## Introduction

Resonance is an important and useful phenomenon in almost every field of physics. And yet, in the field of surface acoustic waves, a resonant element was conspicuously lacking for most of the period since 1967 when rapid advances were being made in many other aspects of the field. This peculiar condition was due to the frustrating fact that a simple, "perfect" reflector (analogous to the electric wall in electromagnetics) for the most commonly used Rayleigh mode does not exist, or has not yet been discovered. Rather than reflecting all of the Rayleigh wave, such simple discontinuities as sharp corners at the edge of a substrate reflect only partially and at the same time convert a large fraction of the Rayleigh-wave energy into bulk modes which radiate into the substrate.

At this Symposium in 1970, Ash[1] proposed the use of reflection gratings (periodic arrays of many weakly-reflecting individual elements) as a solution to the reflection problem that would ultimately lead to the high-performance resonators available today. Unfortunately, the experimental results presented in his paper were somewhat disappointing, and the virtue of his proposal did not receive the attention that it warranted. No further work on SAW resonators was to appear in the literature until 1974, when Staples[2], unaware of Ash's earlier work, independently conceived of the same solution to the reflection problem and was able to experimentally obtain Q's of $10^4$ at 140 MHz.

The unique feature of SAW resonators, as typified by Staples results, and which has generated so much interest[3], is their ability to achieve in a very small device Q's of the order of tens of thousands from 60 MHz up to the lower GHz range. The availability of such high-Q resonators allows the extension to a higher frequency range of well-established techniques employed for frequency control and filtering at lower frequencies by means of bulk-crystal resonators. At the same time, there is the possibility of implementing many sophisticated microwave-filter designs in miniature form.

Despite the differences in physical appearance between the SAW resonator and the conventional waveguide cavity, there are many conceptual similarities in the physics of these devices. Furthermore, the same microwave-network techniques employed in the analysis of electromagnetic waveguide resonators are equally applicable to the SAW resonator and are widely used. Problems of SAW propagation in uniform and periodic structures, and of scattering from discontinuities, can all be phrased in terms of distributed and lumped equivalent networks which serve to translate the problem into terms familiar to the microwave engineer.

The purpose of the present paper is to discuss the physical properties of the basic resonator, drawing some analogies to conventional waveguide resonaotrs, to review its loss mechanisms and the limitations on Q imposed by these losses.

* Sponsored by the Department of the Air Force.

## Analogies Between SAW and Microwave Resonator Geometries

The basic SAW resonator consists of two (narrowband) grating reflectors separated by an appropriate gap which permits the constructive interference of successive reflections of a surface-wave beam between the reflectors. (The reflection gratings may be viewed as periodic structures which are operated in their lowest ($\pi$) stop band, where the grating period is approximately half the Rayleigh wavelength.) Such a resonator, using gratings of finite length, will experience some leakage of energy through the imperfectly reflecting gratings, which are analogous to the coupling irises of a waveguide cavity. A schematic of the basic SAW resonator is shown in Fig. 1(b), which also includes transducers used to excite the cavity from outside, without perturbing the basic resonator. This configuration is therefore analogous to the two-port microwave transmission cavity. The analogue of the loop-coupled reflection cavity is shown in Fig. 1(a), in which a transducer is positioned as a coupling element inside the cavity. In this configuration, the input reflection coefficient of the coupling transducer undergoes a classic rapid variation in magnitude and phase in the vicinity of resonance. (As in the case of the loop, the introduction of the transducer results in a perturbation of the resonant cavity which must be accounted for in a careful design.) Similarly, one can place two coupling transducers inside the cavity in the manner of Fig. 1(c), to form the analogue of the loop-coupled transmission cavity having a narrowband filter response. In each of the above cases, the qualitative behavior of the SAW device closely parallels that of its electromagnetic counterpart. Certain differences in detail do, however, exist and these are due primarily to the narrowband nature of the grating reflector, whose properties will be briefly reviewed in the next section.

## The SAW Grating Reflector

The grating reflector produces a strong surface-wave reflection by the coherent superposition of many weak reflections from individual reflecting elements. The latter may consist of various kinds of strips deposited on the surface, material implanted in the surface, or grooves etched in the surface[3]. In the remainder of this paper, the behavior of the grooved reflector and resonator are chosen to illustrate the properties of this class of device.

Figure 2 shows the cross section of an uniform array of shallow rectangular grooves in a substrate surface, and also shows the equivalent network for such an array[4], which is valid as long as bulk-scattering and diffraction losses are negligible. The narrowband nature of the grating reflector is evident from Fig. 3, which shows the magnitude and phase of the reflection coefficient $\Gamma$ for an array of 200 grooves on a Y-Z $LiNbO_3$ substrate, as calculated at the reference planes $T_1$ or $T_2$, using the equivalent network of Fig. 2. In Fig. 3, the horizontal frequency axis is normalized to the "center" frequency, $f_0$=v/2d, where v is the surface-wave velocity on the unperturbed surface and d is the array period. It is apparent from Fig. 3 that the array reflects most strongly at a frequency $\hat{f} < f_0$, which is to be expected from the fact that the wave on a capacitively-loaded periodic transmission line is slower than that on a uniform line. Furthermore, for this $LiNbO_3$ substrate, the phase of $\Gamma$ is seen to be $\pi/2$ radians at $\hat{f}$, which corresponds to the existence of a voltage minimum at the edge of the first groove.

It should be emphasized at this point that the incident energy penetrates a considerable distance into the distributed reflector, consistent with the small stop-band attenuation which is characteristic of the arrays employed. It therefore follows that resonators using such reflectors store a large proportion of their energy within the distributed reflectors, a condition which does not have a parallel among conventional waveguide resonators which use localized reflectors. The penetration of energy into the reflector region is measured by the phase slope of the reflection coefficient[3,4].

In addition to the main lobe of $\Gamma$, there are the usual sidelobes characteristic of a finite array, but $|\Gamma|$ associated with these sidelobes is in general much smaller, and therefore not useful for high-Q resonators. Instead of being a liability, however, the narrowband nature of $\Gamma$ actually serves the useful function of suppressing the other allowed resonances which lie away from the main-lobe peak. In so doing, the grating reflector acts as a built-in mode-selection filter.

## Frequency Response of Basic Grooved Resonators

In order to maximize the Q of a resonator for a given grating reflector, the resonance should be designed to coincide with $\hat{f}$, where $|\Gamma|$ is a maximum. To this end, it is first necessary to know $\hat{f}$ accurately, and then to separate the grating reflectors by a distance measured between the first-groove edges (short-circuit planes) of $L = n\hat{\lambda}/2$, $n = 1, 2, 3 \ldots$, where $\hat{\lambda} = v/\hat{f}$ is the wavelength corresponding to $\hat{f}$ on the free surface. When designed in this way, the basic resonator (Fig. 1(b) exhibits a sharp transmission peak at $\hat{f}$ in the center of the grating stop band.

The equivalent network for the basic resonator is very simply constructed by connecting the equivalent networks for the two separate gratings (Fig. 2) by a uniform length of line corresponding to the grating separation. Using this equivalent network, the calculated transmission loss is shown in Fig. 4 (transducer loss not included) for a 68 MHz resonator in which 200-groove reflectors are separated by $L = 10\hat{\lambda}$. The grooves are 3% of a wavelength in depth, and the width-to-space ratio of the array is unity. Transmission is almost complete outside the grating stop band where the reflectors are essentially "transparent", decreases rapidly as the stop band is encountered, and then peaks suddenly as resonance occurs. The Q cited in the inset of Fig. 4 is the standard bandwidth Q, or acoustic loaded Q, defined as

$$Q_L = f_r/\Delta f \qquad (1)$$

where $f_r$ is the resonant frequency and $\Delta f$ is the 3-dB bandwidth. Analogous to the conventional transmission cavity, the transmission loss at resonance can be cast in the familiar form[5]:

$$\tau = 20 \log_{10} \frac{Q_r}{Q_L} \text{ (in dB)} \qquad (2)$$

where $Q_r$ is the radiation Q associated with leakage loss through the imperfect reflectors[3].

Although the configuration of Fig. 1(b) is useful for examining the properties of the basic resonator, the out-of-band response exhibited in Fig. 4 is clearly undesirable from the standpoint of a narrowband transmission filter, for which the configuration of Fig. 1(c) is much more appropriate[3].

## Limits of Achievable Q

As with any type of resonator, the Q of the surface-wave resonator is a function of its various losses. Ultimately, if all other loss mechanisms could be made vanishingly small, the Q of the resonator would be limited by the intrinsic (surface-wave) propagation loss of the substrate. The latter includes contributions from viscous damping loss as well as the air-loading loss due to energy radiated into the air region adjoining the substrate surface. The air-loading loss can be eliminated by sealing the resonator in an evacuated package so that the viscous loss is the ultimate limiting factor on Q. The Q of the resonator due to propagation loss alone is termed the material Q, $Q_m$. A calculation of $Q_m$ for the commonly used substrates of Y-Z $LiNbO_3$ and ST quartz is shown in Fig. 5 for both air-loaded and evacuated conditions. According to these curves, material losses impose a ceiling on Q of approximately $10^5$ at 100 MHz. The effect of propagation losses on resonator performance is included by the use of a complex propagation constant in the equivalent network.

Another fundamental type of loss mechanism is that due to diffraction of the finite-width beam, as it propagates back and forth between the reflectors. As the beam spreads, part of the energy "spills" beyond the aperture of the reflector and is lost to the system. Fortunately, however, diffraction loss can be minimized as much as desired by increasing the beam width. Defining a diffraction Q, $Q_d$, due to this loss, it can be shown that $Q_d$ is proportional to the square of beam width[6]. Values of $Q_d$ for a typical beam width of $50\lambda$ are also given in Fig. 5, which shows that on ST quartz the ceiling on Q is set by diffraction loss rather than propagation loss for a $50\lambda$ beam at frequencies below 200 MHz. The preceding conclusions regarding diffraction loss are based on the assumption of propagation on a uniform surface. In fact, however, much of the resonator surface is not uniform, but is perturbed by periodic grating regions, which may result in a type of waveguiding. For a discussion of the implications of such loading for the diffraction loss, the reader is referred to Ref. 3.

A potential source of loss is the leakage through the imperfectly reflecting ($|\Gamma|<1$) gratings. This leakage loss is a function of the details of the reflector, namely, the number of elements (grooves in this case) therein, the reflection coefficient of each element, and the width-to-space ratio of the element. The radiation Q, $Q_r$, associated with this leakage loss is inversely proportional to $(1-|\Gamma|^2)$ (Ref. 7). Details of the dependence of $Q_r$ for a grooved resonator on the grating parameters may be found in Ref. 4 and 8.

Another source of loss in the resonator is due to mode conversion into radiating bulk waves[8]. Since diffraction loss can in principal be made negligible by increasing the beam width, the attainment of the material Q depends on the ability to design a grating which minimizes leakage loss without incurring significant bulk-scattering loss at the grating edges. An indication of the feasibility of attaining $Q_m$ on the important temperature-stable ST cut of quartz is shown in Fig. 6, in which theory is compared with measurement of acoustic loaded Q, $Q_L$, in air and in vacuum, on several grooved resonators with different groove depths[8]. For the two deepest cases, evacuation resulted in an increase in Q of roughly 70%, indicating that air-loading loss was a significant limitation, and that leakage and bulk-scattering losses were indeed minimal. These experiments indicate that grooved grating reflectors can be designed such that leakage and bulk-scattering losses do not limit the achievement of the material Q on ST quartz.

## Conclusion

High-Q SAW resonators have opened the way for the miniaturized realization in the VHF to lower GHz range, of coupled-resonator filters and resonator-stablized oscillators. The existence of accurate equivalent networks casts the problem into a form which is readily amenable to analysis and synthesis via well-established microwave-network techniques (see following paper in this session). Given the individual resonators described above, one can conceive of many different ways to couple them them together, either electrically or acoustically, but the optimum coupling scheme for achieving useful filter responses remains an open issue. To this end, microwave-network techniques and insights also provide a useful guide.

## References


1. E.A. Ash, Microwave Symp.Digest, 385-386, May 1970.
2. E.J. Staples, Proc. 28th Ann. Frequency Control Symp., 280-285; May 1974.
3. For a review article containing extensive and current references on the subject of SAW resonators, see: D.T. Bell, Jr., and R.C.M. Li, IEEE Proc., Special Issue on SAW Technology, May 1976.
4. R.C.M. Li, J.A. Alusow, and R.C. Williamson, Proc. 29th Ann. Frequency Control Symp., 167-176; May 1975.
5. R.C.M. Li, unpublished result.
6. R.C.M. Li, et al, Ultrason.Symp.Proc.,257-262, 1974.
7. E.J. Staples, et al, Ultrason.Symp.Proc.,245-252, 1974.
8. R.C.M. Li, et al, Ultrason. Symp. Proc.,279-283; 1975.


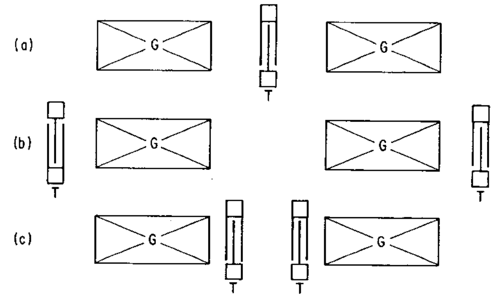


Fig.1 Surface-wave analogue of: a) loop-coupled reflection cavity, b) iris-coupled transmission cavity, and c) loop-coupled transmission cavity.

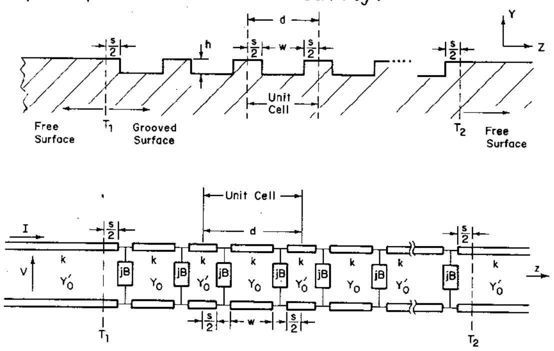


$Y_0'/Y_0 \simeq 1 - C_1\frac{h}{\lambda}$ $B/Y_0 \simeq C_2\left(\frac{h}{\lambda}\right)^2$

For Y-Z $LiNbO_3$: $C_1 \simeq \frac{2}{3}$, $C_2 \simeq 42$

Fig.2 Equivalent network for grooved reflection grating.

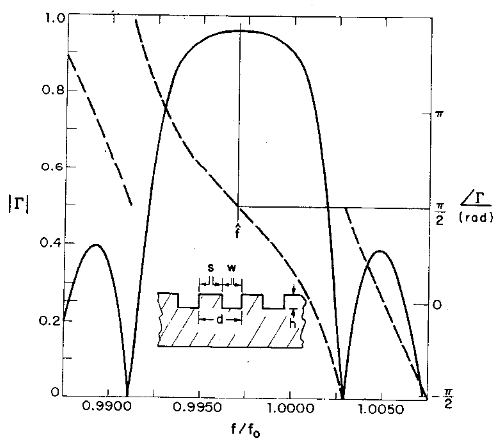


Fig.3 Magnitude and phase of reflection coefficient (at reference planes $T_1$ or $T_2$ of Fig. 2) for reflection grating of 200 grooves (h/2d = 0.015, w/s = 1.0) on Y-Z $LiNbO_3$.

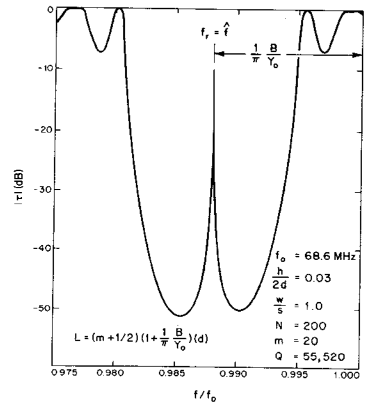


Fig.4 Calculated transmission through basic $LiNbO_3$ resonator of 200-groove reflectors (h/2d = 0.03, w/s = 1.0) separated by 10λ at 68 MHz.

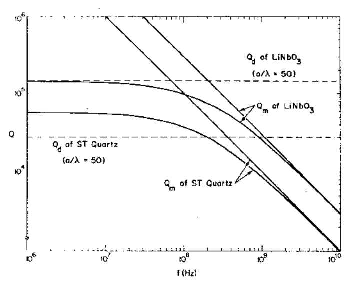


Fig.5 Material and diffraction Q's for Y-Z $LiNbO_3$ and ST quartz. Curved and straight lines for $Q_m$ correspond to air-loaded and evacuated conditions, respectively.

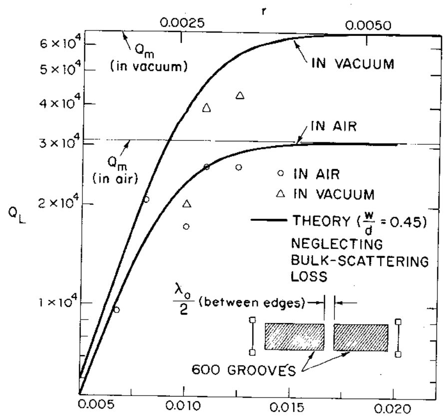


Fig.6 Comparison of measurement and calculation of acoustic loaded Q at 157 MHz for resonators on ST quartz having 600 grooves per grating.